International Journal of Heat and Fluid Flow 63 (2017) 99–107

Contents lists available at ScienceDirect

International Journal of Heat and Fluid Flow

journal homepage: www.elsevier.com/locate/ijhff

A numerical study of a plane wall jet with heat transfer

Iftekhar Z. Naqavi*, James C. Tyacke, Paul G. Tucker

Department of Engineering, University of Cambridge, Cambridge, UK

ARTICLE INFO

Article history:
Available online 3 August 2016

Keywords:
Wall jet
Heat transfer
Direct numerical simulation (DNS)
Prandtl number
Turbulent Prandtl number

ABSTRACT

A direct numerical simulation (DNS) of a wall jet is performed at $Re = 7500$. To the authors' knowledge, this is the highest Reynolds number DNS study of a wall jet. The heat transfer process is studied with an iso-thermal boundary condition at the wall. The molecular Prandtl number is $Pr = 0.71$. Mean flow and heat transfer parameters are contrasted with available measurements and Nusselt number coefficient correlations. The scaling parameters for heat transfer variables are investigated. The mean temperature $\langle T\rangle$, temperature root mean square T_{rms}, streamwise $\langle u'T'\rangle$ and wall normal $\langle v'T'\rangle$ heat flux profiles show collapse in the streamwise direction, with the inner scaling, the outer scaling and the thermal scaling parameters. The complete budgets for temperature variance $\langle T'T'\rangle$ and turbulent heat fluxes are also presented.

1. Introduction

A high momentum fluid issuing from a narrow slot along a flat plate forms a wall jet. The near wall region, called the inner layer, acts like a turbulent boundary layer flow. The region away from the wall, called the outer layer, acts like a free shear flow. Due to its practical applications in film cooling for gas turbine blades and boundary layer control on high lift airfoils it has been studied extensively, Launder and Rodi provide a review of the state of the art until 1983 in Launder and Rodi (1983). Determination of self-similar behaviour in wall jets is important for turbulence modelling. The required eddy viscosity depends on the different flow regions and uncertainties in turbulent statistics have been found to be high (Launder and Rodi, 1983). It has been shown by George et al. (2000) that with appropriate scaling, velocity and Reynolds stress profiles collapse at infinitely large Reynolds number. There are two different scalings for the two wall jet regions, namely, the inner and outer scaling. These are presented in Fig. 1. For the inner layer, friction velocity u_τ and ν/u_τ are the velocity and length scales. The outer scaling parameter for the velocity is the local maximum mean streamwise velocity U_{max} and for the wall normal distance it is $y_{1/2}$, which is the wall normal distance of a point where the mean streamwise velocity $\langle u\rangle$ is half of the U_{max}. In the outer layer, Reynolds shear stress scales with friction velocity u_τ^2, whereas normal stresses and mean velocities scale with maximum velocity U_{max}.

Several studies with measurements and simulations are available, investigating the flow physics of wall jets (Launder and Rodi, 1983). The heat transfer from an isothermal wall, which is an important aspect of the wall jet applications, has received little attention. There is significant variation in suggested constants for log-law ($\frac{1}{\kappa}\ln y^+ + A$) type flow behaviour in planar wall jets (for example $0.41 < \kappa < 0.6$ and $5 < A < 6.8$ (Banyassady and Piomelli, 2015)) and this poses a problem for flow and thermal predictions and measurements. Ahlman et al. (2007) performed a DNS of a wall jet with scalar transport, at a relatively lower Reynolds number of 2000 to study inner and outer scalings showing self similarity behaviour at several downstream locations. Banyassady and Piomelli (2015) use LES and joint probability density functions to assess the level of influence of the outer layer on the inner. They conclude an independent scaling at infinite Reynolds number and a larger scaling overlap region as local Reynolds number decreases as suggested by George et al. (2000). For a $Re = 9600$ wall jet, Dejoan and Leschziner (2005) compute turbulence budgets and realizability maps highlighting turbulent stresses, length and time scales to differ substantially from channel flows. These are important turbulence modelling aspects. They employ LES, finding minor subgrid model effects on an 8 million cell mesh. Dacos et al. (1984) measured temperature, heat fluxes and the triple-velocity-temperature product for a plane wall jet with isothermal boundary conditions. They note that over 90% of the temperature change from the wall is effected in the inner layer and compare temperature profile scalings using wall coordinates. For a planar wall jet, AbdulNour et al. (2000) measure the convective heat transfer coefficient. The authors focus on the developing flow region at smaller axial distances ($0 < x/h < 13$) for automotive defroster applications. Insensitivity

* Corresponding author.
E-mail address: izn20@eng.cam.ac.uk (I.Z. Naqavi).

http://dx.doi.org/10.1016/j.ijheatfluidflow.2016.07.012
0142-727X/© 2016 Published by Elsevier Inc.

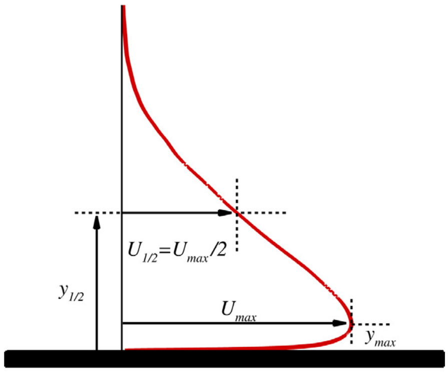

Fig. 1. Parameters for inner and outer scaling.

to the thermal boundary condition was found at locations ($5 \leq x/h$), where the outer layer has diffused into the inner jet. A minimum in heat transfer coefficient is also found at $x/h \approx 5$. The correlation between the turbulence and heat transfer processes is also poorly understood. Pouransari et al. (2015) study the effect of passive and reactive scalar fields on the anisotropy of a wall jet using DNS. Anisotropy is accentuated near the wall but persists throughout the wall jet. Strong intermittency and anisotropy persistence at small scales is hence a challenge to predict.

In the current work a direct numerical simulation of a plane wall jet is performed to investigate the heat transfer process from an isothermal wall. The simulations are conducted at a significant Reynolds number, $Re = 7500$ for which Rostamy et al. (2011) have performed flow measurements. The emphasis in this paper is on the scaling properties of the flow and heat transfer variables. In addition to the inner and outer scaling for heat transfer variables, the so called thermal scale is also considered. In thermal scaling, the thermal half width $y_{\theta/2}$ is defined as the wall normal distance of a point where the temperature is half of the maximum local temperature. The results for velocity field, turbulent heat flux and their budgets will also be discussed and contrasted with other flows and literature.

2. Simulation details

The wall jet is simulated with the conservation of mass and momentum equations for unsteady three dimensional incompressible flow:

$$\frac{\partial u_j}{\partial x_j} = 0 \tag{1}$$

$$\frac{\partial u_i}{\partial t} + \frac{\partial u_j u_i}{\partial x_j} = -\frac{\partial p}{\partial x_i} + \frac{1}{Re}\frac{\partial^2 u_i}{\partial x_j \partial x_j}; \tag{2}$$

where $\{x_1, x_2, x_3\} = \{x, y, z\}$ are the coordinates in the streamwise, wall-normal and spanwise directions, respectively. $\{u_1, u_2, u_3\} = \{u, v, w\}$ are the corresponding instantaneous velocities. p is the instantaneous pressure. $Re = U_j h/\nu$ is the Reynolds number based on the jet velocity U_j, the jet slot height h and the molecular viscosity ν.

Heat transfer is simulated with a scalar transport equation:

$$\frac{\partial T}{\partial t} + \frac{\partial T u_i}{\partial x_i} = \frac{1}{RePr}\frac{\partial^2 T}{\partial x_i \partial x_i}, \tag{3}$$

where T is the non-dimensional instantaneous temperature and Pr is the molecular Prandtl number. The non-dimensional temperature is defined as $T = \frac{\theta-\theta_\infty}{\theta_w-\theta_\infty}$, whereas θ is the physical temperature, θ_w is the wall temperature and θ_∞ is the temperature of the incoming fluid at the inlet plane. These governing equations are discretised with a second-order, collocated, finite volume solver. The solver is based on fractional step scheme, which uses semi-implicit time advancement. The scalar convection term is discretized with the QUICK (Quadratic Upstream Interpolation for Convective Kinetics) scheme (Leonard, 1979). Further details of numerical methods and examples of application of this code can be found in previous publications (Radhakrishnan et al., 2006; Naqavi et al., 2014).

The computational domain has the dimensions of $L_x/h = 43.0, L_y/h = 40.0$ and $L_z/h = 9.0$ in the streamwise, wall-normal and spanwise directions, respectively. At the inflow plane a velocity profile is specified for the wall jet up to $y/h = 1.0$ and the rest of the plane has a uniform co-flow of $0.06U_j$. This uniform co-flow provides the fluid for the jet entrainment. The lower wall obeys the no slip and impermeability conditions. The upper boundary has a free slip boundary condition and a periodic condition is applied in the spanwise direction. At the outflow plane a convective boundary condition is applied as $\frac{\partial u_i}{\partial t} + U_{conv}\frac{\partial u_i}{\partial x}$. The convective velocity U_{conv} is the mean streamwise velocity at the outflow plane. It is calculated as a running average. The initial transients are eliminated with weighted averaging in time given as;

$$U_{conv}^{n+1} = \frac{\Delta t}{W_t}\langle u^n\rangle_z + \left(1 - \frac{\Delta t}{W_t}\right)U_{conv}^n, \tag{4}$$

Δt is the time step size, n is the number of time step, $\langle\,\rangle_z$ represents the spanwise averaging and W_t is the averaging weight. When the simulation is started from a uniform flow, $W_t = 10$ for initial $t^* = tU_j/h = 200$ time units. Once the flow is developed, $W_t = 100$ is used for the next $t^* = 500$ time units. Finally, a simple running time average is used to calculate U_{conv}^{n+1};

$$U_{conv}^{n+1} = U_{conv}^n + (U_{conv}^n - \langle u^n\rangle_z)/n. \tag{5}$$

At the jet inlet plane, Rostamy et al. (2011) did not provide any mean or turbulent velocities. Hence, based on the inlet configuration (Fig. 2(*a*)) given by Rostamy et al. (2011), a precursor RANS calculation is used to calculate the mean inlet velocity profile. To add small, time dependent perturbations at the inlet, a separate channel flow simulation is used. The channel dimensions are $2\pi h \times h \times \pi h$, in the streamwise, wall-normal and spanwise directions, respectively. The periodic condition is defined in the streamwise and spanwise directions and no-slip condition at the top and bottom wall of the channel. The channel flow Reynolds number is $Re_{channel} = \frac{U_{bulk}h}{\nu} = 7500$. The mean channel flow velocity is removed from the instantaneous channel flow field and the remaining fluctuations are scaled to give a turbulence intensity of less than 0.1%. These fluctuations are superimposed on the RANS velocity profile. These help to initiate shear layer transition in the wall jet. Fig. 2(*b*) shows the resulting profiles of the mean velocity and Reynolds stress in the streamwise direction at the jet inlet.

The heat transfer Eq. (3) is solved for temperature T, with a periodic boundary condition in the spanwise direction. A uniform temperature $T_\infty = 0.0$ is defined at the inlet plane. A convective boundary condition, as described previously for the flow equations, is used at the outflow plane. The lower wall has the isothermal condition of $T_w = 1.0$ and the upper wall is adiabatic. The Reynolds number is $Re = 7500$ and the Prandtl number is $Pr = 0.71$ for the current simulations. The domain is discretized with $1652 \times 344 \times 302$ grid points in the streamwise, wall-normal and spanwise directions, respectively, giving a total of 172 million cells. Fig. 3(*a*) shows the grid spacing in wall units, based on local friction velocity, along the streamwise direction, with a maximum of $\Delta x^+ < 10.5$, $\Delta y^+ < 0.7$ and $\Delta z^+ < 12.0$. The Δy grid varies in both streamwise and wall-normal direction to follow the spreading of the jet. The contours of Δy^+ in Fig. 3(*b*) show that the maximum $\Delta y^+ < 10.0$ in the active flow region. There are six points below $y^+ = 5$ and twelve points below $y^+ = 11$. The simulation is performed for $t^* = 1300$ time units to remove the initial transients. The statistics are collected for next $t^* = 1200$ time units.